Physics in Medicine & Biology

IPEM Institute of Physics and Engineering in Medicine

NOTE

A practical method for quantifying dose in bone and lung using TLDs when using 6 and 15 MV photon beams

Neslihan Sarigul[1,5], Murat Surucu[2,5], Chester Reft[3], Martha Malin[3], Zehra Yegingil[4] and Bulent Aydogan[3,6]

[1] Institute of Nuclear Science, Hacettepe University, 06532 Ankara, Turkey
[2] Department of Radiation Oncology, Loyola University Medical Center, Maywood, IL 60660, United States of America
[3] Department of Radiation and Cellular Oncology, University of Chicago Pritzker School of Medicine, Chicago, IL 60637, United States of America
[4] Arts-Sciences Faculty, Physics Department, Cukurova University, 01330, Adana, Turkey
[5] Both authors contributed equally to this manuscript.
[6] Author to whom any correspondence should be addressed.

E-mail: nsarigul@hacettepe.edu.tr, msurucu@lumc.edu, creft@radonc.uchicago.edu, mmalin@radonc.uchicago.edu, zehra@cukurova.edu.tr and baydogan@radonc.uchicago.edu

Abstract

This paper presents a practical method for converting dose measured with thermoluminescent dosimeters (TLD) to dose in lung and bone for 6 MV and 15 MV photon beams. Monte Carlo (MC) simulations and Burlin cavity theory calculations were performed to calculate $f_{\mathrm{medium}}^{\mathrm{TLD}}$, the dose-to-TLD to dose-to-medium conversion factor. A practical method was proposed for converting TLD-measured-dose to dose-in-medium using the TLD dose calibration in water and $f_{\mathrm{water}}^{\mathrm{medium}}$, dose-to-medium to dose-to-water conversion factor. Theoretical calculations for $f_{\mathrm{water}}^{\mathrm{medium}}$ were performed using photon spectrum weighted parameters and were compared with MC simulations. Verification of the proposed method was done using phantoms having either bone or lung equivalent slabs stacked in between solid water slabs. Percent depth dose (PDD) curves were measured using 0.089 cm thick LiF:Mg,Ti (TLD-100) dosemeters placed at various depths within these phantoms. They were then corrected with $f_{\mathrm{water}}^{\mathrm{medium}}$ factors using the proposed dose conversion method, and were compared with the MC simulations. For 6 MV beam, the MC calculated $f_{\mathrm{water}}^{\mathrm{medium}}$ factors were 0.942 and 1.002 for bone and lung, and for 15 MV it was 0.927 and 1.005 for bone and lung, respectively. The difference between the MC simulated and spectrum weighted theoretical $f_{\mathrm{water}}^{\mathrm{medium}}$ factors were within 3% for both lung and bone. The PDD curves measured with TLD-100 chips that were corrected using the proposed method agreed well within 1.5% of the MC simulated PDD curves for both the water/lung/water and water/bone/water (WBW) phantoms. The dose-to-medium correction using MC simulated $f_{\mathrm{water}}^{\mathrm{medium}}$ is convenient, easy, and accurate. Therefore, it can be used instead of Burlin cavity theory, especially in media with high atomic numbers such as bone for accurate dose quantification.

1. Introduction

TLDs are preferred due to their near tissue equivalence, low signal fading (5%–10% per year), wide linear response range (10 μGy–10 Gy); and high sensitivity for very low dose measurements (Chen and Leung 2001, Montaño-García and Gamboa-deBuen 2006). Their small size allows point dose measurements in phantoms as well as for *in vivo* dosimetry on patients during radiotherapy treatment (Hsi *et al* 2013). Although there are a few small detectors that can be used to measure dose such as Markus chamber, one advantage of using TLDs would be that multiple different locations can be verified in one irradiation using multiple TLDs conveniently. For instance, it is accustomed that after verifying the treatment planning system (TPS) beam model in homogenous medium, heterogeneous phantoms are used to further test the accuracy in more clinically relevant scenarios. One type of these anthropomorphic heterogeneous phantoms are Alderson–Rando phantom, which includes small holes for TLD measurements to mimic clinical situations can be placed (Surucu *et al* 2012). Moreover, there are

some clinical situations where TLDs may provide a convenient solution for complex problems such as *in vivo* measurement of dose at the rectal wall during proton treatment by simply integrating in an endorectal balloon or intraoperative electron radiation therapy (Hsi *et al* 2013, Liuzzi *et al* 2015).

Although a large fraction of human body is composed of water, inhomogeneities, especially the cortical bone due to its high effective atomic number (Z), present challenges in dose measurement, calculation, verification, and interpretation of the results. A rigorous TPS commissioning must include verification of dose to medium (D_{medium}) in bone and lung as well. D_{medium} in radiation experiments, clinical verifications, and treatment planning commissioning validation is generally measured with TLDs. Having similar effective atomic numbers, TLD-100 chips can be used to report the dose-to-water (D_{water}) and likewise dose-to-lung using Bragg-Gray cavity theory. The difficulty, however, is with measuring dose in medium with high effective atomic numbers like cortical bone for which Burlin cavity theory is suggested to be more appropriate. Bragg-Gray cavity theory assumes that a small size detector will not disturb the radiation fluence, where this assumption is quite difficult satisfy for medium size cavities (Dewerd 2009). Burlin cavity theory requires the parameter d, the fraction of dose contribution resulting from photon interactions in the phantom material, to convert D_{water} to D_{medium}; nevertheless, it is very difficult at best to determine the accurate d value for TLD-100 (Nariyama and Tanaka 1997). Most of the studies focusing on measuring and or calculating D_{medium} did not include any details for converting dose measured in TLD-100 chips to D_{medium}. One particular reason may be the difficulty of calculating parameters required in this conversion and lack of reference for an accurate yet practical dose conversion method. The aim of this study is to investigate a practical method to allow accurate convert TLD-100 measured dose (D_{TLD}) to D_{medium} conversion in lung and bone for 6 MV and 15 MV clinical photon beams using Burlin cavity theory and MC simulation. The dose conversion method established in this study was verified using a clinical setup that is generally employed during validation of TPS commissioning. The PDD in water/bone/water (WBW) and water/lung/water (WLW) slab phantoms were measured with TLD-100 chips. The dose measured by TLD-100 chips were then converted to D_{medium} in bone and lung using the proposed dose conversion method and compared with the MC simulated D_{medium} for these slab phantoms.

2. Materials and methods

Being a relative dosimeter, TLD-100 chips require calibration using a known dose in a medium. TG-51 protocol (Almond *et al* 1999) provides a methodology to determine the dose in water, which is typically used to calibrate the TLD-100 chips for radiotherapy applications. Dose to medium conversion can be simplified using the approach presented below. The f factors to convert the dose in TLD-100 to that in water or medium (f_{water}^{TLD}, f_{medium}^{TLD}) can be written as follows:

$$f_{water}^{TLD} = \frac{(D_{TLD})^{in\ water}}{D_{water}} = \frac{(R_{TLD})^{in\ water}\ k_{TLD}}{D_{water}} \tag{1}$$

$$f_{medium}^{TLD} = \frac{(D_{TLD})^{in\ medium}}{D_{medium}} = \frac{(R_{TLD})^{in\ medium}\ k_{TLD}}{D_{medium}} \tag{2}$$

where R_{TLD} is the TLD-100 reading and k_{TLD} gives the relation between the light emitted from the TLD-100 and mean absorbed dose, i.e., Gray per unit TLD-100 light that is specified by intrinsic properties of the specific TLD-100 and it is independent of the surrounding medium, for the energies studied herein. D_{medium} will then be:
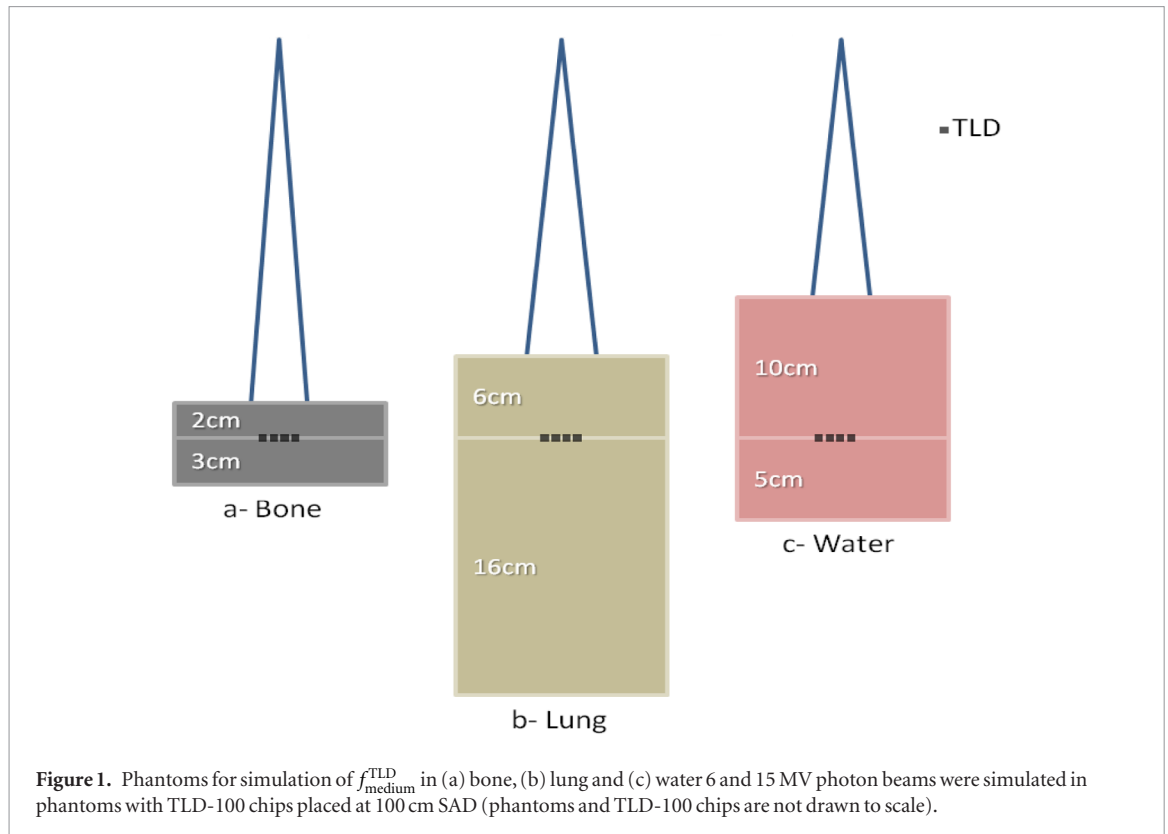
$$D_{medium} = D_{water}\ \frac{f_{water}^{TLD}}{f_{medium}^{TLD}}\ \frac{(R_{TLD})^{in\ medium}}{(R_{TLD})^{in\ water}}. \tag{3}$$

Finally, f_{water}^{medium} is the simple ratio as defined below and can be calculated either using the Burlin cavity theory or MC methods.

$$f_{water}^{medium} = f_{water}^{TLD}/f_{medium}^{TLD} \tag{4}$$

2.1. Monte Carlo Simulations

Unlike conventional TPSs, MC dose calculation programs report dose-to-medium and are suggested to be the golden standard. MC have been long used for accurate estimation of absorbed dose in or near heterogeneities (Haraldsson *et al* 2003, Ma and Li 2011). In this study, we used EGSnrc (Electron Gamma Shower, National Research Council Canada) MC simulation program in order to calculate dose in medium and also the cavity to medium dose conversion factor f_{medium}^{TLD}. Three virtual phantoms (shown in figure 1) were constructed, in EGSnrc. The 6 MV beam reference phase space data generated for Varian Clinac 2100 Linac (Varian Medical Systems Inc., Palo Alto, California) by Cho *et al* (2005) using BEAMnrc code (Rogers *et al* 2011) was used in this

Figure 1. Phantoms for simulation of $f_{\text{medium}}^{\text{TLD}}$ in (a) bone, (b) lung and (c) water 6 and 15 MV photon beams were simulated in phantoms with TLD-100 chips placed at 100 cm SAD (phantoms and TLD-100 chips are not drawn to scale).

study. For 15 MV simulations, vendor supplied phase space data for Varian TrueBeam Linac was used. The field size was $10 \times 10\,\text{cm}^2$ and DOSXYZnrc (Walters *et al* 2013) was used to calculate dose distribution in phantoms. Four TLD-100 chips were placed in equivalent bone, lung or water slabs at 100 cm SAD (Source-to-axis distance). The bone phantom had 2 cm of bone, the lung phantom had 6 cm of lung and water phantom had 10 cm of water equivalent buildup with adequate slabs of same material for backscatter. The depths of TLD-100 chips were chosen such that corresponding water equivalent depths were beyond the depth of maximum dose (d_{max}).

Slab phantom materials were selected as H2O521ICRU, LUNG521ICRU and ICRPBONE521ICRU for water, lung and bone, respectively. TLD-100 is widely used to measure dose in radiotherapy clinics, has a density of $2.64\,\text{g cm}^{-3}$, and is LiF doped with Mg and Ti (LiF:Mg,Ti). Mobit *et al* (1998) showed that doping has minimal effect on mass collision stopping-power or mass energy-absorption coefficient; hence, LiF instead of LiF:Mg,Ti was used to represent TLD-100 in MC calculations. In order to calculate the dose conversion factor, *f*, dose-to-medium in the absence of the cavity is required (equation (2)) which can be simulated using MC methods. Therefore, a separate simulation for each medium was performed without TLD-100 chips to calculate the dose-to-medium at the exact TLD-100 locations. The ratio of the TLD-100 registered dose to the dose-to-medium is then used to calculate the *f* factors. The TLD-100 dimensions were $0.32 \times 0.32 \times 0.089\,\text{cm}^3$. The voxel size used in MC simulations varied according to the location in the phantom with finer resolution where the doses were scored. It was $0.032 \times 0.032\,\text{cm}^2$ in the plane perpendicular to the beam axis with a thickness of 0.008 cm along the central axis. As such, each TLD-100 used in this study was divided into $10 \times 10 \times 11$ voxels. The $f_{\text{medium}}^{\text{TLD}}$ was calculated on a voxel-by-voxel basis to eliminate the effect of any beam quality changes, and then averaged over all the 1100 voxels corresponding to each TLD-100. Electron transport was terminated at 10 keV (ECUT = 0.521 MeV) and the creation of delta rays above this cut-off was explicitly simulated (AE = 0.521 MeV). The photon transport cut-off was set to 10 keV and the creation of bremsstrahlung photons with energy above 10 keV was also explicitly simulated (AP = PCUT = 10 keV). The fractional energy loss per electron step was set to 2.5% (ESTEPE = 0.025). Typically, 5×10^8 histories were used in the MC simulations to achieve an uncertainty less than 1%. The PEGS4 material database with cross-sections for total energies down to 0.521 MeV was used for each medium. The NSplit parameter was chosen to be 30 (Walters *et al* 2013). MATLAB (version 2009b, Mathworks, Natick, MA) was used to analyze the MC dose distributions.

2.1.1. Field size and depth dependency of f factors

By definition *f* values is expected to be independent of field size (FS) and depth as long as the charged particle equilibrium exists. To verify, we have performed virtual experiments using the phantom shown in figure 1(a) for $2 \times 2\,\text{cm}^2$, $4 \times 4\,\text{cm}^2$ and $10 \times 10\,\text{cm}^2$ FS. Additional MC simulations were done at depths of 1 cm and 3 cm in bone, 3 cm and 12 cm in lung and, 5 cm and 10 cm in water to study the depth dependency.
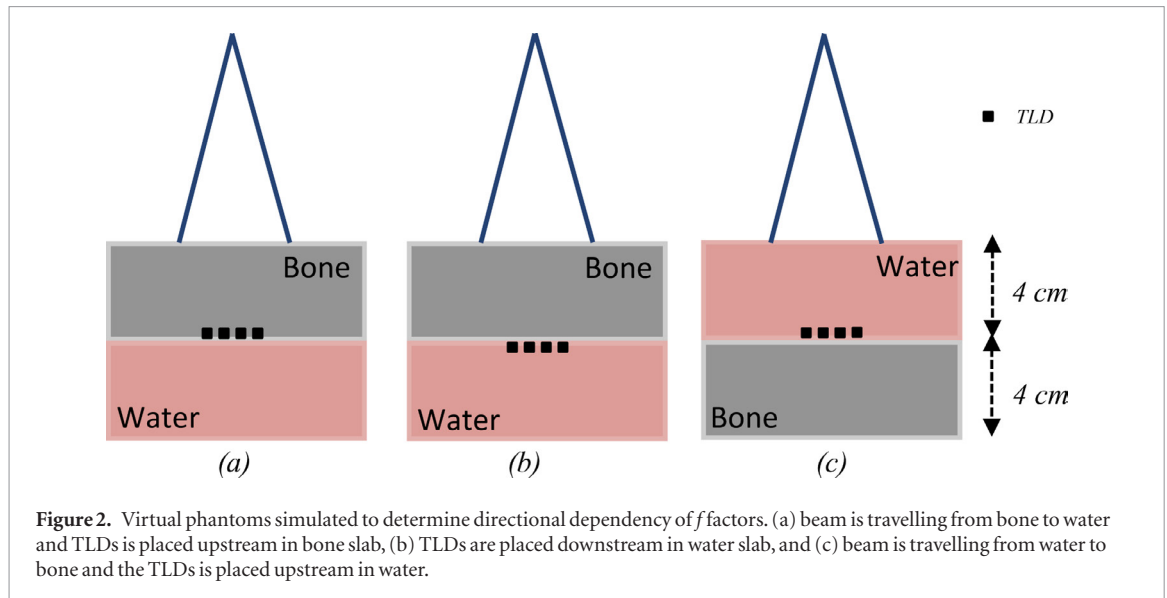
Figure 2. Virtual phantoms simulated to determine directional dependency of *f* factors. (a) beam is travelling from bone to water and TLDs is placed upstream in bone slab, (b) TLDs are placed downstream in water slab, and (c) beam is travelling from water to bone and the TLDs is placed upstream in water.

2.1.2. Directional dependency of f factors.

Three virtual phantoms shown in figure 2 were simulated to study the directional dependency of *f* values. DOSXYZnrc (Walters *et al* 2013) was used to simulate the dose distribution in phantoms as explained in previous sections. Four TLD-100 chips were placed in equivalent bone or water slabs at the junctions of water and bone slabs either upstream in bone (figure 2(a)), downstream in water (figure 2(b)) and upstream in water (figure 2(c)) The simulations are done at 96 cm source to surface distance and $10 \times 10 \, \text{cm}^2$ FS for each configuration.

2.2. Theoretical calculations

2.2.1. Bragg-Gray cavity theory

A detector is placed in a medium, forms a cavity in that medium (Mobit *et al* 1997). The cavity is usually made of a material that has a different atomic number and density than the medium. TLD represents cavity. Bragg–Gray cavity theory relates the absorbed dose in a medium D_{medium} and the average absorbed dose in the cavity (D_{TLD}) in small cavities as following (Carlsson 1985, Horowitz 1982):

$$f_{\text{medium}}^{\text{TLD}} = \frac{D_{\text{TLD}}}{D_{\text{medium}}} = \left(\frac{s}{\rho} \right)_{\text{medium}}^{\text{TLD}} \tag{5}$$

where $f_{\text{medium}}^{\text{TLD}}$ is the dose-to-TLD to dose-to-medium conversion factor and $\frac{s}{\rho}_{\text{medium}}^{\text{TLD}}$ is the ratio of mean mass collisional stopping power of the cavity to that of the medium.

2.2.2. Burlin cavity theory

Cavity theory assumes that the cavity should be small with respect to the range of most secondary electrons (small cavity). For a cavity that is much larger than the range of the most energetic electrons, cavity material determines the electron spectrum within it. The problem arises when the range of electrons are comparable or larger than the cavity size, and one solution for this was proposed by Burlin (1966) and Kearsley (1984) as follows;

$$f_{\text{medium}}^{\text{TLD}} = \frac{D_{\text{TLD}}}{D_{\text{medium}}} = d \left(\frac{s}{\rho} \right)_{\text{medium}}^{\text{TLD}} + (1 - d) \left(\frac{\mu_{en}}{\rho} \right)_{\text{medium}}^{\text{TLD}} \tag{6}$$

where $\frac{\mu_{en}}{\rho}_{\text{medium}}^{\text{TLD}}$ is the ratio of average mass energy absorption coefficients of the cavity to the medium. The weighting factor *d*, varies between unity for small (or Bragg–Gray) cavity and zero for large cavity. The parameter *d* is the fraction of dose contribution resulting from photon interactions in the phantom material (Burlin 1966, Paliwal 1975, Haider *et al* 1997). It accounts for the attenuation of electrons across the cavity and is calculated using the following formula (Attix 1986);

$$d \equiv \frac{\overline{\phi_m}}{\phi_m^e} = \frac{1 - e^{-\beta g}}{\beta g} \tag{7}$$

$$1 - d \equiv \frac{\overline{\phi_c}}{\phi_c^e} = \frac{\beta g + e^{-\beta g} - 1}{\beta g} \tag{8}$$

where, $\overline{\Phi_m^e}$ and $\overline{\Phi_m}$ are the mean electron fluence in medium with and without charge particle equilibrium, respectively. The dose component resulting from photon interactions in the cavity, $1 - d$, is equal to the ratio of the electron fluence created by the photons in the cavity to that created under electronic equilibrium (Silva 1989). The average path length of electrons across the cavity or the mean cord length, g, is often determined using the following formula (Burlin and Chan 1969).

$$g = \frac{4V}{S}\rho \tag{9}$$

where, V is the cavity volume and S is the surface area of the cavity. r is calculated for electrons passing through the volume and not generated in the volume. The parameter β describes the effective mass attenuation coefficient of the electrons penetrating the cavity material that originate from the wall (Burlin 1966, Ogunleye 1980) and it was determined using equation (10) formulated by Janssens *et al* (1974) where R is the extrapolated range for the maximum energy of the secondary electrons (Silva 1989, Scarboro and Kry 2013).
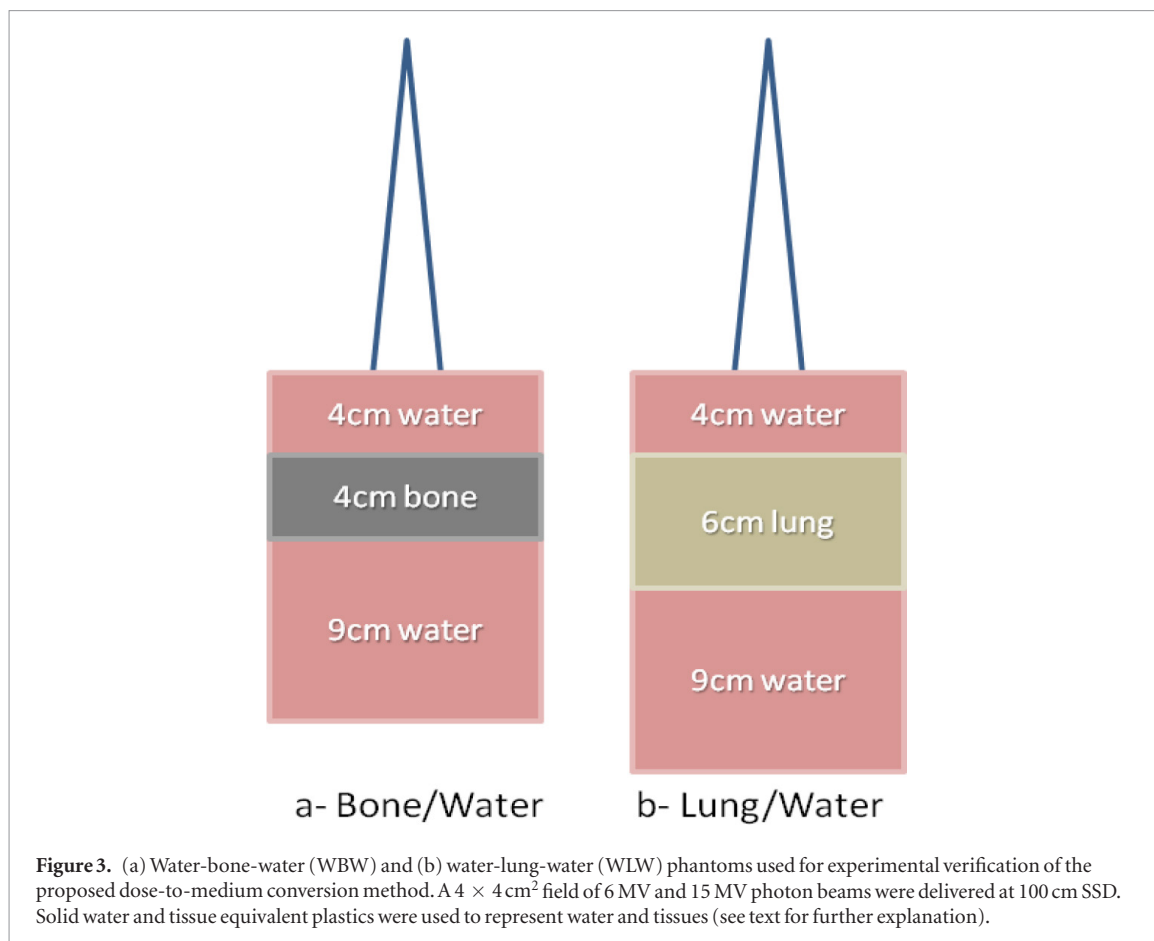
$$e^{-\beta R} = 0.04. \tag{10}$$

Photon and electron spectrum in bone, lung, and water was analyzed in order to determine the spectrum weighted $\frac{\mu_{en}}{\rho}\frac{\text{TLD}}{\text{medium}}$, $\frac{s}{\rho}\frac{\text{TLD}}{\text{medium}}$, and β values. The electron and photon spectrum for three virtual phantoms shown in figure 1 were analyzed at the depth of TLD-100 chips using EGSnrc BEAMdp. The photon spectrum was divided into 10 bins and the corresponding $\frac{\mu_{en}}{\rho}\frac{\text{TLD}}{\text{medium}}$ values were obtained from NIST (Hubbell and Seltzer 1995). The spectrum averaged $\frac{\mu_{en}}{\rho}\frac{\text{TLD}}{\text{medium}}$ values were then calculated for TLD-100 chips in bone, lung, and water phantoms, separately. The electron spectrum at the depth of TLD-100 chips in each phantom was divided into 25 bins, and $\frac{s}{\rho}\frac{\text{TLD}}{\text{medium}}$ and the R values were obtained from NIST (Berger *et al* 1999) for each corresponding energy bin. The spectrum weighted average values of $\frac{s}{\rho}\frac{\text{TLD}}{\text{medium}}$ and the R values were calculated for each phantom, separately. According to Burlin (Burlin and Chan 1969) the parameter g depends on the density and the dimensions of TLD (equation (9)). The parameter d was calculated using equations (7)–(10) in order to compute the f factors. The ratio of the $f_{\text{water}}^{\text{TLD}}$ to $f_{\text{medium}}^{\text{TLD}}$ was then used to calculate $f_{\text{water}}^{\text{medium}}$ factors for both the bone and lung. The theoretical calculations differ from the MC simulations in the way that the parameter d, $\frac{\mu_{en}}{\rho}\frac{\text{TLD}}{\text{medium}}$ and $\frac{s}{\rho}\frac{\text{TLD}}{\text{medium}}$ are required for the calculation of $f_{\text{medium}}^{\text{TLD}}$ whereas the latter can be directly simulated using MC methods from the doses scored with and without the TLD-100 chips at the same point in medium.

2.3. Experimental validation

The standard annealing procedure as recommended by the manufacturer was used before using the TLD-100 chips. TLD-100 chips were annealed in high temperature Fisher Scientific Isotemp Oven (Fisher Scientific, Pittsburgh, PA) at 400 °C for one hour to minimize the residual TL signal by emptying the high temperature traps and to restore the original sensitivity and glow curve structure. After the high temperature annealing, the chips were left for fast cooling to room temperature by placing the tray on a brass block. After 30 min, they were then annealed at 80 °C for 20–24 h in low temperature TLD Annealing Furnace 120 VAC (Radiation Product Design, Inc. Albertville, MN. Item number: 168-001) to reduce fading through minimization the contribution of the low temperature peaks. And they were again rapidly cooled to room temperature, where they were kept at least 16–24 h. All TLD-100 chips were irradiated four times under consistent conditions to determine a relative sensitivity for each dosimeter in order to determine the 'best' TLDs to use. The irradiations were done in 10 cm depth solid water phantom which was 10 cm water equivalent material, followed by 5 cm water equivalent material. The TLDs were performed using 10x10 cm2 field size of the 6 MV photon beam with 115 and 150 MU dose. TLD readouts were performed using a Harshaw QS 5500 (Termo Scientific) type reader. TLD-100 chips were analyzed according to the protocol described by Reft *et al* (2006). Individual TLD-100 sensitivities were determined to reduce the measurement uncertainties to better than $\pm 1.5\%$ (1 SD).

An experimental setup used during our recent TPS commissioning was employed to verify the accuracy of the proposed dose conversion method herein. Figure 3 shows the experimental slab phantom geometries for both bone (4 cm solid water, 4 or 4.5 cm cortical bone, and 9 cm solid water slabs) and lung (4 cm solid water followed by 6 cm lung and 9 cm solid water slabs). The composition of the lung-equivalent material was 8.5% H, 59.4% C, 2.0% N, 18% O, 0.1% Cl, 0.8% Si, 11.2% Mg by weight, with an average density of 0.30 g cm^{-3}. The bone equivalent material was composed of 3.4% H, 31.4% C, 1.8% N, 36.5% O, and 26.8% Ca with an average density of 1.85 g cm^{-3}. Composition of the tissue equivalent plastic materials was provided by Gammex, Inc.

Each slab was modified to have three small cutout sections for the placement of TLD-100 chips. The 0.089 cm thick TLD-100 chips were placed at various depths, in the central axis, including the interfaces between the water and bone or water and lung in order to measure the percent depth dose (Percent depth dose) curves. Three TLD-100 chips were placed at the depths of 1 cm, 1.5 cm, 3.5 cm and 10 cm in solid water and 4.5 cm, 5.5 cm, 6.5 cm, 7.5 cm and 8.5 cm in bone equivalent plastic. The three TLD-100 chips at each depth were placed within 5 mm

Figure 3. (a) Water-bone-water (WBW) and (b) water-lung-water (WLW) phantoms used for experimental verification of the proposed dose-to-medium conversion method. A $4 \times 4\,cm^2$ field of 6 MV and 15 MV photon beams were delivered at 100 cm SSD. Solid water and tissue equivalent plastics were used to represent water and tissues (see text for further explanation).

and were irradiated simultaneously. The small possibility of them affecting each other was ignored. Similarly, three TLD-100 chips were placed at the water-bone interfaces at the depth of 4 cm and 8 cm. Three TLD-100 chips at each depth were placed inside the water-lung-water phantom at eight different depths (1, 1.5, 4, 6, 8, 10, 11, 13 cm) along the central axis. A $4 \times 4\,cm^2$ field was irradiated with 6 and 15 MV beams. TLD-100 measurements were repeated three times in order to reduce the statistical uncertainty. The dimension of lung and bone phantoms were $30 \times 30 \times 20\,cm^3$, and $30 \times 30 \times 17\,cm^3$, respectively. D_{water} conversion for TLD-100 measured dose was carried out by delivering a known dose at reference geometry (using the TG 51 protocol) in solid water, after applying a correction factor to account for the water versus solid water difference, similar to the one described by Seuntjens *et al* (2005). The TLD-100 readings were then converted to D_{medium} using Bragg-Gray cavity theory and the f_{water}^{medium} calculated both the Burlin cavity theory and the MC methods. The measured PDD curves were also compared with the ones obtained using MC methods. The same MC parameters described above were used to simulate a total of 8×10^8 histories in order to achieve less than 1% statistical uncertainty.

3. Results

Table 1 displays the f_{medium}^{TLD} factors simulated with MC and calculated with Burlin cavity theory for bone, lung, and water, which were used to compute the f_{water}^{medium}. Theoretically calculated f factors agreed with the ones simulated using MC methods within 1.3% for 6 MV and 3% for 15 MV. Better agreement was observed for 6 MV and in lung and water than for higher energy 15 MV beam in high Z bone.

3.1. Field size and depth dependency
Figure 1 was used to test field size and depth dependency of f factors. When the field size was changed from $2 \times 2\,cm^2$ to $10 \times 10\,cm^2$ the f factors differed less than 0.5%. To determine the depth dependency, f factor simulation was carried out at the depths of 1 cm and 3 cm in bone, 3 cm and 12 cm in lung and 5 cm and 10 cm in water phantoms shown in figure 1. The maximum difference in f value was 1.2%.

3.2. Directional dependency
It is expected that the f values to exhibit a directional dependency in the boundaries of heterogeneities as the spectrum of scattered electrons changes. The f values were 0.89 when the TLDs were placed in the bone slab upstream in figure 2(a) and reduced to 0.836 when they were placed downstream in the water (figure 2(b)). This

Table 1. Comparison of f factors for bone and lung simulated by MC and calculated using Burlin cavity theory (equation (6)) for 0.089 cm thick TLD-100.

		Monte Carlo	Burlin	%difference (MC-Burlin) (%)
6 MV	$f_{\text{bone}}^{\text{TLD}}$	0.892% ± 0.8%	0.892% ± 3.5%	0.0
	$f_{\text{lung}}^{\text{TLD}}$	0.838% ± 0.7%	0.836% ± 3.5%	0.2
	$f_{\text{water}}^{\text{TLD}}$	0.840% ± 0.8%	0.829% ± 3.5%	1.2
	$f_{\text{water}}^{\text{bone}}$	0.942% ± 0.9%	0.929% ± 4.5%	1.3
	$f_{\text{water}}^{\text{lung}}$	1.002% ± 1.0%	0.992% ± 4.5%	1.0
15 MV	$f_{\text{bone}}^{\text{TLD}}$	0.918% ± 0.9%	0.890% ± 3.5%	3.0
	$f_{\text{lung}}^{\text{TLD}}$	0.847% ± 0.9%	0.849% ± 3.5%	0.3
	$f_{\text{water}}^{\text{TLD}}$	0.851% ± 0.9%	0.842% ± 3.5%	1.1
	$f_{\text{water}}^{\text{bone}}$	0.927% ± 1.0%	0.946% ± 4.5%	1.8
	$f_{\text{water}}^{\text{lung}}$	1.005% ± 0.9%	0.992% ± 4.5%	1.3

is mainly due to the interaction and dose deposition characteristic of high energy photons in high Z medium versus low Z medium. When the phantom shown in figure 2(c) is flipped to have the beam travel from water to bone but keeping the TLDs still in the water, the f values increased to 0.846 due to increased backscatter from bone.
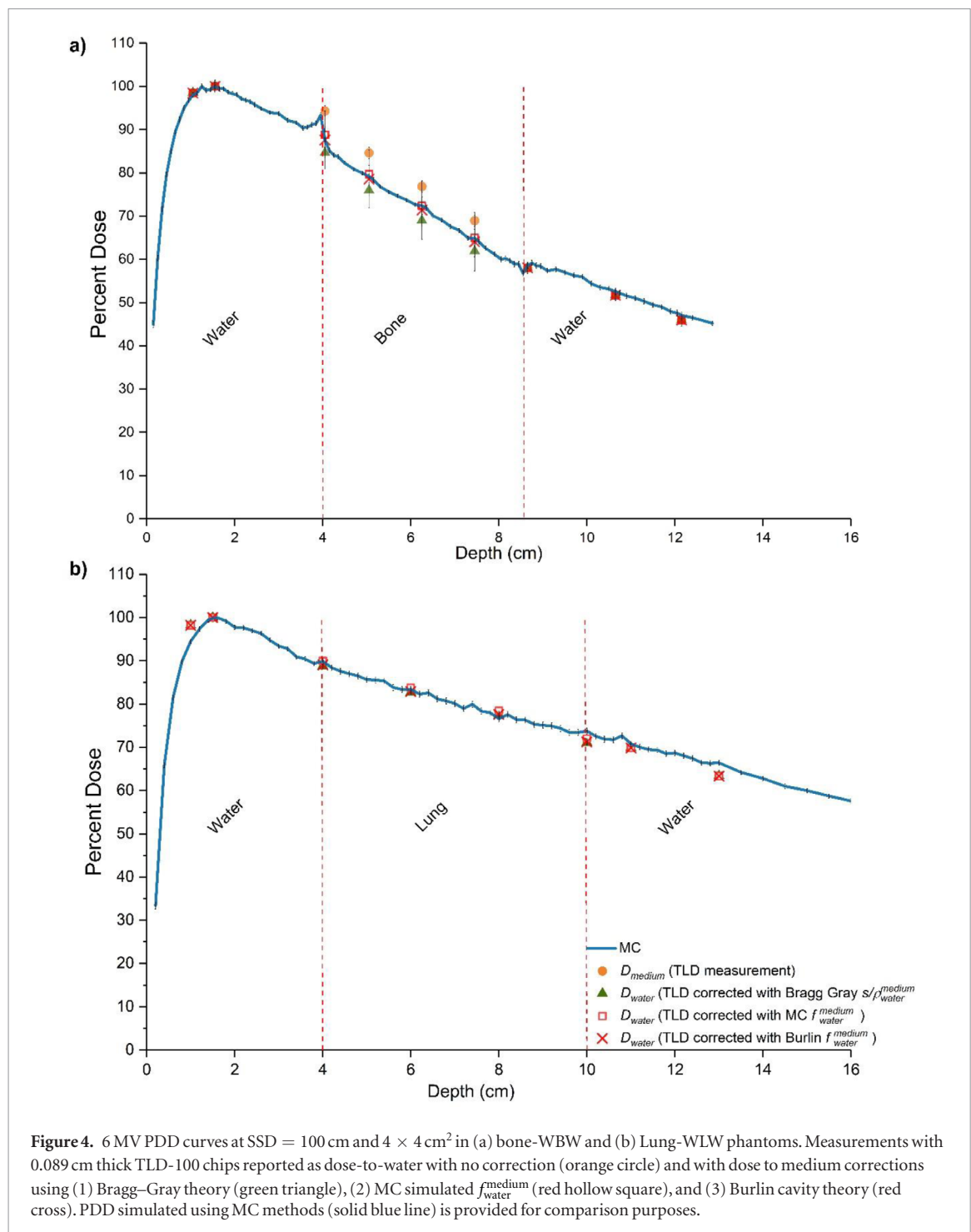
3.3. Uncertainty estimates

Uncertainties associated both with the MC simulations and theoretical calculations were presented in table 1. Uncertainties for the theoretical f factors can be attributed to the Type B uncertainties associated with the NIST provided mass energy absorption coefficients (Hubbell 1982) (~2%) and mass collision stopping power (Seltzer and Berger 1984) (~1%) as well as the assumptions in the estimates of β, g and d parameters. Maximum uncertainties associated with the theoretical calculations were greater than 3.5% with a maximum value of 4.5%. Type A uncertainties associated with the MC spectrum analysis simulations were calculated through history-based relative statistical uncertainty estimation. Each TLD-100 was divided into $10 \times 10 \times 11$ voxels, the standard deviation of dose in each TLD-100 was calculated from the values in all voxels within the TLD-100. The combined standard uncertainties obtained using summation in quadrature and reported as one standard deviation. Number of histories is adjusted accordingly to obtain a maximum uncertainly of 1% associated with MC simulations in this study. Total uncertainty associated with of the determination of was carried out by including all possible sources of uncertainties from TLD-100 measurements to determination of f factors to dose conversion. Uncertainty in TLD-100 sensitivity was measured to be less than 1.5%. The uncertainty in the charge-to-dose calibration was estimated to be around 2% and the uncertainty in the determination of d_{max} including slab thickness and SSD was accepted about 1%. Maximum uncertainty associated with MC simulations f factors was 1% in both WLW and WBW phantoms, whereas 4.5% with the theoretical calculations. Adding these uncertainties in quadrature resulted in a total uncertainty in D_{medium} of approximately 2.5% and 5% using the proposed method herein with the f factors obtained MC simulations and Burlin cavity theory, respectively.

Total uncertainty associated with D_{medium} was twice as much when using theoretical f factors calculated using the less than the one associated with the theoretical f factor calculation by its convert. Therefore, MC simulated $f_{\text{water}}^{\text{medium}}$ was used to determine D_{medium}, i.e. convert dose to water measured using TLD-100 chips to dose to medium in the proposed method. Shown in figures 4 and 5 are the Percent depth doses for the WBW and WLW phantoms depicted in figure 3.
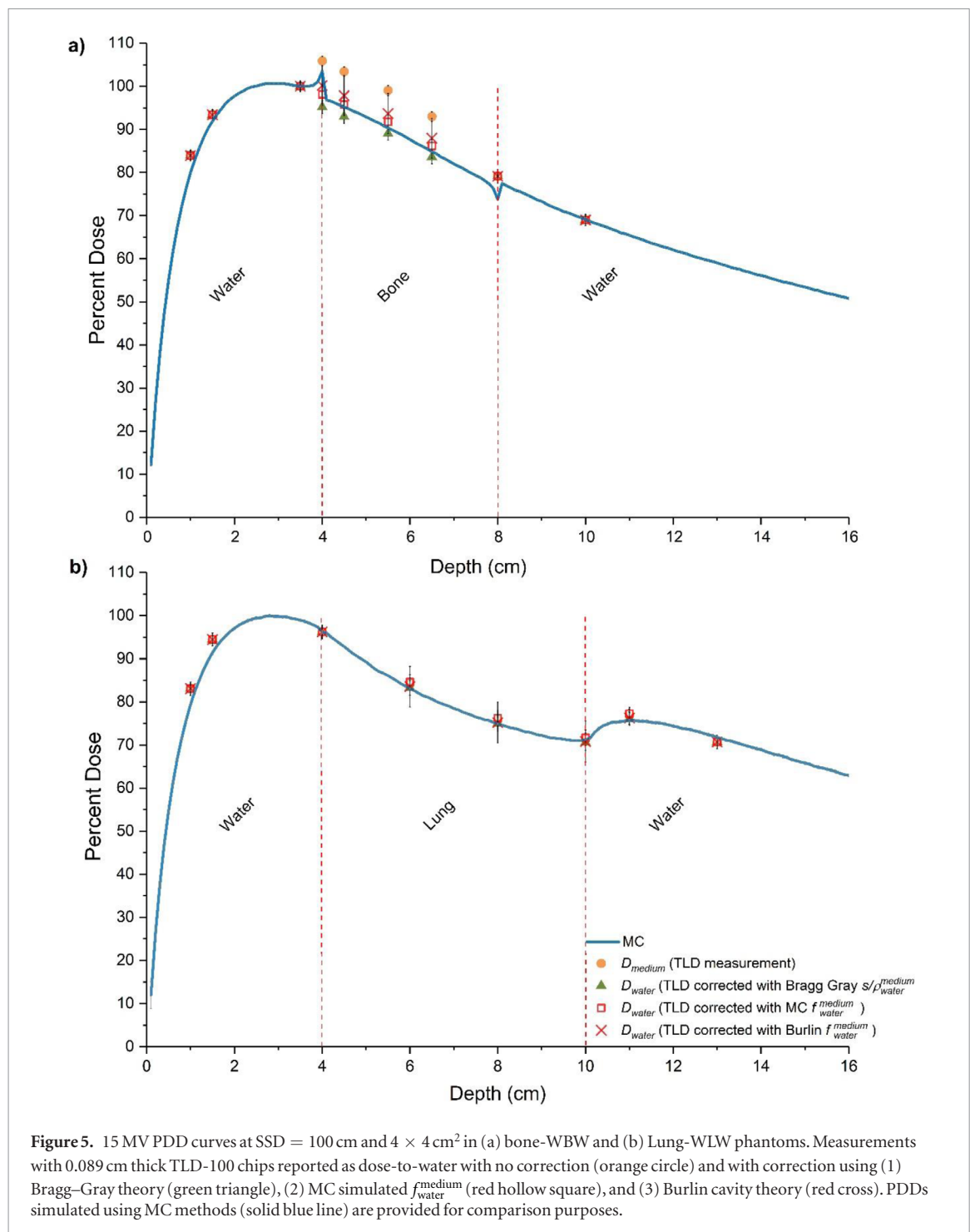
3.4. PDDs for WBW and WLW

Figures 4 and 5 compares the PDDs for 6 MV and 15 MV, respectively, obtained using (1) MC simulations (blue solid line), (2) TLD-100 measurements dose to water (orange ball), (3) TLD-100 measurements corrected by the Bragg-Gray cavity theory (red cross), (4) TLD-100 measurements corrected by the $f_{\text{water}}^{\text{medium}}$ using the proposed method herein using the MC simulations (red square), and (5) TLD-100 measurements corrected with Burlin cavity theory. The agreement in PDDs between all four methods was within 1% in lung. In bone, on the other hand, Bragg–Gray theory underestimated the dose by ~5%, while TLD-100 doses corrected with $f_{\text{water}}^{\text{medium}}$ agreed within 1%. The measurements at the interface have a greater uncertainty because of the dose contributions from both medium and can only be captured by MC. Since the TLD-100 chips were housed in the holes drilled inside bone slab at the proximal water/bone interface at 4 cm depth, the corrections were applied to the result of this TLD-100 measurement. Whereas for TLD-100 chips at the distal bone/water interface at 8 cm depth were housed inside the solid water phantom as such were not corrected.

Figure 4. 6 MV PDD curves at SSD = 100 cm and 4 × 4 cm^2 in (a) bone-WBW and (b) Lung-WLW phantoms. Measurements with 0.089 cm thick TLD-100 chips reported as dose-to-water with no correction (orange circle) and with dose to medium corrections using (1) Bragg–Gray theory (green triangle), (2) MC simulated f_{water}^{medium} (red hollow square), and (3) Burlin cavity theory (red cross). PDD simulated using MC methods (solid blue line) is provided for comparison purposes.

Shown in figure 5 are PDDs for 15 MV obtained using MC simulations are the TLD-100 measurements corrected by; (1) the mass collision stopping power ratios using Bragg–Gray cavity theory, (2) the f_{water}^{medium} (table 1) determined using both the proposed method in this study using the MC simulations and Burlin cavity theory. Dose correction with the Bragg-Gray theory underestimated the dose around ~3% in bone, while the MC simulated and the f_{water}^{medium} corrected TLD-100 doses agreed within 1%. As expected, the agreement in lung was around 1% between the MC calculations, Burlin and Bragg-Gray theory. The measurements at the interface have a greater uncertainty because of the dose contributions from both medium and can only be captured by MC. Since the TLD-100 chips were housed in the holes drilled inside bone slab at the proximal water/bone interface at 4 cm depth, the corrections were applied to the result of this TLD-100 measurement. Whereas for TLD-100 chips at the distal bone/water interface at 8 cm depth were housed inside the solid water phantom as such were not corrected.

Dose correction with the Bragg-Gray theory underestimated the dose around ~5% in bone for 6 MV, while the MC simulated and the f_{water}^{medium} corrected TLD doses agreed within 1%. As expected, the agreement in lung was around 1% between the MC calculations, Burlin and Bragg–Gray theory. The measurements at the interface have

Figure 5. 15 MV PDD curves at SSD = 100 cm and 4 × 4 cm^2 in (a) bone-WBW and (b) Lung-WLW phantoms. Measurements with 0.089 cm thick TLD-100 chips reported as dose-to-water with no correction (orange circle) and with correction using (1) Bragg–Gray theory (green triangle), (2) MC simulated $f_{\text{water}}^{\text{medium}}$ (red hollow square), and (3) Burlin cavity theory (red cross). PDDs simulated using MC methods (solid blue line) are provided for comparison purposes.

a greater uncertainty because of the dose contributions from both medium and can only be captured by MC. Since the TLD-100 chips were housed in the holes drilled inside bone slab at the proximal water/bone interface at 4 cm depth, the corrections were applied to the result of this TLD-100 measurement. Whereas for TLD-100 chips at the distal bone/water interface at 8 cm depth were housed inside the solid water phantom as such were not corrected.

4. Discussion and conclusions

Measurement of dose in heterogeneous media is a classical problem in radiotherapy and investigated widely using MC simulations and theoretical calculations. It is common to use the first order approach to convert dose in TLD-100 to dose in medium using mass collision stopping power ratios as suggested by Bragg–Gray cavity theory. This approach provides correct estimates for lung, however, not for high Z media such as cortical bone. This can be attributed to the fact that the TLD-100 chips, having similar effective Z, will not disturb the charge

particle fluence that would have existed if the cavity and the surrounding medium were of the similar material. For high Z materials such as bone, however, TLD-100 chips having a low effective Z will perturb the charge particle fluence. Also, the range of secondary electrons will be much shorter in a high Z and high-density medium like bone. As a result, TLD-100 chips will behave less like a small cavity, disturbing the charge particle fluence and resulting in Bragg–Gray cavity theory to fail. Hence, the correction using mass collision stopping power ratios will not provide accurate results especially in high Z medium. With further increasing the size of the detector or the Z of medium, the charge particle fluence disturbance will increase; as such the determination of D_{medium} will be further complicated.

The TLD-100, due to its small size and its effective Z being very close to water (~8.2, 7.5, and 13.8 for TLD-100, lung and bone, respectively), is commonly employed in radiotherapy to report dose to patient and during TPS commissioning validation particularly for verification of inhomogeneity correction models. It was surprising; however, the manuscripts which reported on the accuracy of the TPS heterogeneity correction models did not discuss the method of converting TLD measured dose to dose-to-medium (Arnfield *et al* 2000, Duch *et al* 2006, Reft *et al* 2006, da Rosa *et al* 2010). Without such explanation dose-to-medium cannot be reported correctly especially for high Z media such as cortical bone. To this end, we systematically analyzed theoretical assumptions in calculating the parameter *d,* which was subsequently employed to calculate the *f* factor in Burlin cavity theory to convert dose-to-TLD in medium to dose-to-medium. We established a dose conversion method to correct TLD-100 measured dose using water calibration doses and calculated the medium to water conversion factor for bone and lung. We tested the proposed method hereinto convert the TLD-100 measured doses to dose in medium, by comparing the measured PDD against MC simulations in phantoms constructed from equivalent bone, lung, and water slabs for 6 and 15 MV clinical photon beams.

One of the advantages of MC simulations is to test and verify the validity of *f* factors for different radiation setups and conditions including depth, location of TLD measurement particularly near junctions, and FS. Cavity theory, on the other hand, neither suggests any possible changes in *f* factors except for different media nor provides a means to verify it. This study demonstrated that the *f* factors are independent of FS and depth supporting the cavity theory prediction where the differences were within the uncertainty of the simulations. Furthermore, *f* factors near junctions of heterogeneities were shown to strongly depend on the medium in which the TLD measurement is done while weakly depend on the location of TLD placement, i.e, upstream or downstream as long as they are placed in the same medium. Nonetheless, these results do not impact or change the results presented in this work in anyways as the both the experimental setup and MC made use of the same exact location for dose comparison purposes, i.e. in the downstream or in deeper medium. Furthermore, the differences in coefficients mainly influence points chosen for dose reporting at the interfaces of inhomogeneities. It is a known fact that measuring or estimating the dose at the interfaces is difficult at the best. Hence, this work focused on the accuracy of dose reporting within the heterogeneous media rather than the doses at the interfaces.

TLDs offer advantages in some clinical situations over other dosimeters including small ionization chambers. Convenience of measuring multiple points during the same irradiation session is important for accuracy and repeatability purposes. This makes the commissioning of TPS especially the inhomogeneity correction when using anthropomorphic phantoms as well as verification of clinically relevant situation easier and may improve accuracy (Surucu *et al* 2012). Recent reports exemplify the versatility of TLDs in complex clinical situations *in vivo* measurement of dose at the rectal wall during proton treatment by simply integrating it in an endorectal balloon or in intraoperative electron radiation therapy (Hsi *et al* 2013, Liuzzi *et al* 2015).

The goal of this work is to provide a practical method to convert TLD measured dose to the dose in medium. It should be noted that there exists an ambiguity in dose reporting in radiation oncology community. Historically, dose is reported as the dose to water (Ma and Li 2011, Andreo 2015, Gladstone *et al* 2016). There are many different implementations of dose calculation algorithms that provide dose to water or dose to medium and it is often vague what exactly an algorithm is computing and reporting. For instance, dose computed to a small volume of water inside the medium is reported as dose to medium (Ma and Li 2011). There are also conceptual and practical concerns over some existing methods to convert from dose to water to dose to medium (Gladstone *et al* 2016). Hence, when using results from this work caution should be exercised. In conclusion, this study provides a much-needed practical method to convert the TLD-100 measured dose to the dose in medium using a MC simulated f_{water}^{medium} factor rather than determining the parameter *d* for a particular TLD-100 using the Burlin cavity theory. This statement is successfully supported through a series of simple experiments, which is commonly used to evaluate the accuracy of heterogeneity corrections during TPS commissioning and validation of dose in heterogeneous medium.

Conflict of interest

The authors have no relevant conflicts of interest to disclose.

References

Almond P R *et al* 1999 AAPM's TG-51 protocol for clinical reference dosimetry of high-energy photon and electron beams *Med. Phys.* **26** 1847–70

Andreo P 2015 Dose to 'water-like' media or dose to tissue in MV photons radiotherapy treatment planning: Still a matter of debate *Phys. Med. Biol.* **60** 309–37

Arnfield M R, Siantar C H, Siebers J, Garmon P, Cox L and Mohan R 2000 The impact of electron transport on the accuracy of computed dose *Med. Phys.* **27** 1266–74

Attix F H 1986 *Introduction to Radiological Physics and Radiation Dosimetry* (New York: Wiley) (https://doi.org/10.1002/9783527617135)

Berger M J, Coursey J S, Zucker M A and Chang J 1999 *ESTAR, PSTAR, and ASTAR: Computer Programs for Calculating Stopping-Power and Range Tables for Electrons, Protons, and Helium Ions* (Gaithersburg: National Institute of Standards and Technology) (https://physics.nist.gov/PhysRefData/Star/Text/ESTAR.html)

Burlin T E 1966 A general theory of cavity ionisation *Br. J. Radiol.* **39** 727–34

Burlin T E and Chan F K 1969 The effect of the wall on the Fricke dosemeter *Int. J. Appl. Radiat. Isot.* **20** 767–75

Carlsson G A 1985 *Theoretical Basis for Dosimetry* (New York: Academic)

Chen R and Leung P L 2001 Nonlinear dose dependence and dose-rate dependence of optically stimulated luminescence and thermoluminescence *Radiat. Meas.* **33** 475–81

Cho S H, Vassiliev O N, Lee S, Liu H H, Ibbott G S and Mohan R 2005 Reference photon dosimetry data and reference phase space data for the 6 MV photon beam from Varian Clinac 2100 series linear accelerators *Med. Phys.* **32** 137–48

Da Rosa L A R *et al* 2010 Percentage depth dose evaluation in heterogeneous media using thermoluminescent dosimetry *J. Appl. Clin. Med. Phys.* **11** 117–27

Dewerd L A, Bartol L J and Davis S D 2009 Chapter 24 thermoluminescence dosimetry (Madison, WI: Medical Physics Publishing)

Duch M A, Carrasco P, Ginjaume M, Jornet N, Ortega X and Ribas M 2006 Dose evaluation in lung-equivalent media in high-energy photon external radiotherapy *Radiat. Prot. Dosim.* **120** 43–7

Gladstone D J, Kry S F, Xiao Y and Chetty I J 2016 Dose specification for NRG radiation therapy trials *Int. J. Radiat. Oncol. Biol. Phys.* **95** 1344–5

Haider J, Skarsgard L D and Lam G K Y 1997 A general cavity theory *Phys. Med. Biol.* **42** 491–500

Haraldsson P, Knöös T, Nyström H and Engström P 2003 Monte Carlo study of TLD measurements in air cavities *Phys. Med. Biol.* **48** N253–9

Horowitz Y S and Dubi A 1982 A proposed modification of Burlin's general cavity theory for photons *Phys. Med. Biol.* **27** 867

Hsi W C, Fagundes M, Zeidan O, Hug E and Schreuder N 2013 Image-guided method for TLD-based *in vivo* rectal dose verification with endorectal balloon in proton therapy for prostate cancer *Med. Phys.* **40** 051715

Hubbell J H 1982 Photon mass attenuation and energy-absorption coefficients *Int. J. Appl. Radiat. Isot.* **33** 1269–90

Hubbell J H and Seltzer S M 1995 *Tables of X-Ray Mass Attenuation Coefficients and Mass Energy-Absorption Coefficients* (Gaithersburg: National Institute of Standards and Technology) (https://www.nist.gov/pml/x-ray-mass-attenuation-coefficients)

Janssens A, Eggermont G, Jacobs R and Thielens G 1974 Spectrum perturbation and energy deposition models for stopping power ratio calculations in general cavity theory *Phys. Med. Biol.* **19** 5

Kearsley E 1984 A general cavity theory *Phys. Med. Biol.* **29** 10

Liuzzi R, Savino F, D'Avino V, Pugliese M and Cella L 2015 Evaluation of LiF:Mg,Ti (TLD-100) for intraoperative electron radiation therapy quality assurance *PLoS One* **10** e0139287

Ma C M and Li J 2011 Dose specification for radiation therapy: Dose to water or dose to medium? *Phys. Med. Biol.* **56** 3073–89

Mobit P N, Nahum A E and Mayles P 1997 An EGS4 Monte Carlo examination of general cavity theory *Phys. Med. Biol.* **42** 1319

Mobit P N, Nahum A E and Mayles P 1998 A Monte Carlo study of the quality dependence factors of common TLD materials in photon and electron beams *Phys. Med. Biol.* **43** 8

Montaño-García C and Gamboa-deBuen I 2006 Measurements of the optical density and the thermoluminescent response of LiF:Mg,Ti exposed to high doses of 60Co gamma rays *Radiat. Prot. Dosim.* **119** 230–2

Nariyama N and Tanaka S 1997 Responses of LiF TLD in different media and cavity ionization theory for low energy photons below 200 keV *J. Nucl. Sci. Technol.* **34** 137–47

Ogunleye O T, Attix F H and Paliwal B R 1980 Comparison of Burlin cavity theory with LiF TLD measurements for cobalt-60 gamma rays *Phys. Med. Biol.* **25** 203–13

Paliwal B R and Almond P R 1975 Applications of cavity theories for electrons to LiF dosemeters *Phys. Med. Biol.* **20** 547–58

Reft C S, Runkel-Muller R and Myrianthopoulos L 2006 *In vivo* and phantom measurements of the secondary photon and neutron doses for prostate patients undergoing 18MV IMRT *Med. Phys.* **33** 3734–42

Rogers D W O, Kawrakow I, Seuntjens J P and Walters B R B 2011 NRC User Codes for EGSnrc (Ottawa: NRC Canada) p 702 (https://nrc-cnrc.github.io/EGSnrc/doc/pirs702-egsnrc-codes.pdf)

Scarboro S B and Kry S F 2013 Characterisation of energy response of Al$_2$O$_3$:C optically stimulated luminescent dosemeters (OSLDs) using cavity theory *Radiat. Prot. Dosim.* **153** 23–31

Seltzer S M and Berger M J 1984 Improved procedure for calculating the collision stopping power of elements and compounds for electrons and positrons *Int. J. Appl. Radiat. Isot.* **35** 665–76

Seuntjens J, Olivares M, Evans M and Podgorsak E 2005 Absorbed dose to water reference dosimetry using solid phantoms in the context of absorbed-dose protocols *Med. Phys.* **32** 2945–53

Silva H 1989 An analysis of the electron spectrum effect on LiF response to cobalt-60 gamma-rays *Nucl. Instrum. Methods Phys. Res.* B **44** 166–71

Surucu M, Yeginer M, Kavak G O, Fan J, Radosevich J A and Aydogan B 2012 Verification of dose distribution for volumetric modulated arc therapy total marrow irradiation in a humanlike phantom *Med. Phys.* **39** 281–8

Walters B, Kawrakow I and Rogers D W O 2013 DOSXYZnrc Users Manual (Ottawa: NRC Canada) (https://nrc-cnrc.github.io/EGSnrc/doc/pirs794-dosxyznrc.pdf)